



# A review on electrical and gas-sensing properties of reduced graphene oxide-metal oxide nanocomposites

Kiranakumar. H. V<sup>1</sup> · Thejas R<sup>1</sup> · Naveen C S<sup>1</sup> · M. Ijaz Khan<sup>2,3,4</sup> · Prasanna G D<sup>5</sup> · Sathish Reddy<sup>6</sup> · Mowffaq Oreijah<sup>7</sup> · Kamel Guedri<sup>7,8</sup> · Omar T. Bafakeeh<sup>9</sup> · Mohammed Jameel<sup>10</sup>

Received: 19 June 2022 / Revised: 11 August 2022 / Accepted: 19 August 2022 / Published online: 3 September 2022  
© The Author(s), under exclusive licence to Springer-Verlag GmbH Germany, part of Springer Nature 2022

## Abstract

From the past decade, there is a demand for the development of highly sensitive and selective, operating at low temperature, and stable gas-sensing materials used to monitor hazardous gases. The discovery of graphene has led to the implication of the same as gas sensor as it possesses large value of surface to volume ratio and high value of electron mobility at room temperature. Few researchers have fabricated reduced graphene oxide–metal oxide composite gas sensors exhibiting good electrical and gas-sensing properties. But still, it is a very less explored area. This article provides an overview of electrical and gas-sensing properties of reduced graphene oxide–metal oxide nanocomposites with improved sensitivity, selectivity, stability, and other sensing performances. This review is mainly focuses on reduced graphene oxide–metal oxide nanocomposite-based gas sensors which are cost-effective and sensitive to the various gases/vapors.

**Keywords** Electrical properties · Gas-sensing properties · Reduced graphene oxide–metal oxide nanocomposites

## 1 Introduction

The development of different types of gas-sensing materials are very important and essential to monitor the gases which are combined into the atmosphere, which leads to several problems for living organisms. Thus, the investigation of

several types of gas sensors are still deficient, to monitor various gases. The nanotechnology is one of the most popular areas for current research and development in all technological disciplines, as the critical dimension scale for devices is now below 100 nm, and it is indeed an ongoing technological revolution in the future [1]. The nanotechnology is

✉ M. Ijaz Khan  
mikhan@math.qau.edu.pk

Naveen C S  
naveen@presidencyuniversity.in

Prasanna G D  
prasannagd@gmail.com

Mowffaq Oreijah  
mmoreijah@uqu.edu.sa

<sup>1</sup> Department of Physics, School of Engineering, Presidency University, Bengaluru, Karnataka 560064, India

<sup>2</sup> Laboratory of Systems Ecology and Sustainability Science, College of Engineering, Peking University, Beijing 100871, People's Republic of China

<sup>3</sup> Mathematical Modelling and Applied Computation Research Group (MMAC), Department of Mathematics, King Abdulaziz University, Jeddah, Saudi Arabia

<sup>4</sup> Department of Mechanical Engineering, Lebanese American University, Beirut, Lebanon

<sup>5</sup> Department of Studies in Physics, Davangere University, Davangere, Karnataka 577007, India

<sup>6</sup> School of Chemical Science, School of Applied Science, Reva University, Bengaluru, Karnataka 560064, India

<sup>7</sup> Mechanical Engineering Department, College of Engineering and Islamic Architecture, Umm Al-Qura University, P.O. Box 5555, Makkah 21955, Saudi Arabia

<sup>8</sup> Research Unity: Materials, Energy and Renewable Energies, Faculty of Science of Gafsa, University of Gafsa, 2100 Gafsa, Tunisia

<sup>9</sup> Department of Industrial Engineering, Jazan University, Jazan 82822, Saudi Arabia

<sup>10</sup> Department of Civil Engineering, College of Engineering, King Khalid University, P. O. Box 960, Asir, Abha Saudi Arabia Postal Code: 61421, Saudi Arabia

used to create, observe, and control matters at the nanometer scale, and is probably in many fields, where in different disciplines, such as physics, chemistry, materials science, biology, and medicine, these are combined to offer immense prospects and challenges and, there is no adverse effect on any part of our lives and living beings. There are various types of nanoparticles reported in many literatures, e.g., metal oxide (MO), mixed metal oxide, polymers, carbon nanotubes (CNT), and graphene oxide (GO) [2–5].

Carbonous materials (CNTs, graphene, fullerenes) have drawn considerable attention from the past three decades due to their exceptional mechanical and electronic properties. Among all carbonous material, graphene is an unpredictable material has a completely distinct, wonderful set of characteristics, which is the structural resemblance of graphite. Graphene is one of the strongest materials ever known to humankind; in contrast, graphite is relatively brittle, and thus it could not be used for structural reinforcement. Graphene is a perfectly two-dimensional material, having excellent crystalline structure and enhanced electrical properties. Graphene was emerged in the short period as a new nanomaterial with the wide variety of applications [6]. Graphene is a one atom thick sheet of carbon, having hexagonal lattice structure (honeycomb crystal lattice structure) as shown in Fig. 1(a), and it is comprising with a densely packed atomically thin layer of  $sp^2$  hybridized material [7]. Graphene can be considered as the thinnest material having a unique combination of characteristics that have the potential applications for the development of future technology. The graphene sheet consists of only trigonally bonded  $sp^2$  carbon atoms, and it is perfectly flat apart from its microscopic ripples. However, GO is a substance made of single

atomic layers that includes carbon, hydrogen, and oxygen molecules as a result of the oxidation of graphite crystals, as seen in Fig. 1(b). GO has two key properties: first, it can be produced using low-cost graphite as the raw material and by using chemical processes with a high yield; second, it is highly hydrophilic and can form stable aqueous colloids, which makes it easier for macroscopic structures to be put together using straightforward and affordable solution processes.

Tetrahedrally bound  $sp^3$  carbon atoms that are slightly displaced above or below the graphene plane make up a portion of the extensively decorated GO sheets, which are atomically rough due to the deformation of the structure and the presence of covalently attached functional groups. Several researchers have studied the surface of GO and observed highly defective regions, probably due to the presence of oxygen, and other areas are nearly intact. Figure 1 depicts the graphene is like honeycomb lattice, and also it is preserved in GO in which the carbon atoms attached to functional groups are slightly displaced, but the overall size of the unit cell in GO remains similar to that of graphene. GO and rGO are hot topics in the research and development of graphene, especially regarding mass applications of graphene. The rGO sheets are often referred to as one kind of chemically produced graphene as shown in Fig. 1(c), and it has also been known by a few other names, such as chemically converted/modified graphene, functionalized graphene, or reduced graphene. The graphene can be obtained from graphite using a solution-assisted or mechanical cleavage exfoliation; rGO is prepared by thermal, hydrothermal, or chemical reduction of GO. A large amount of carbon and oxygen were present in the electrochemically derived rGO

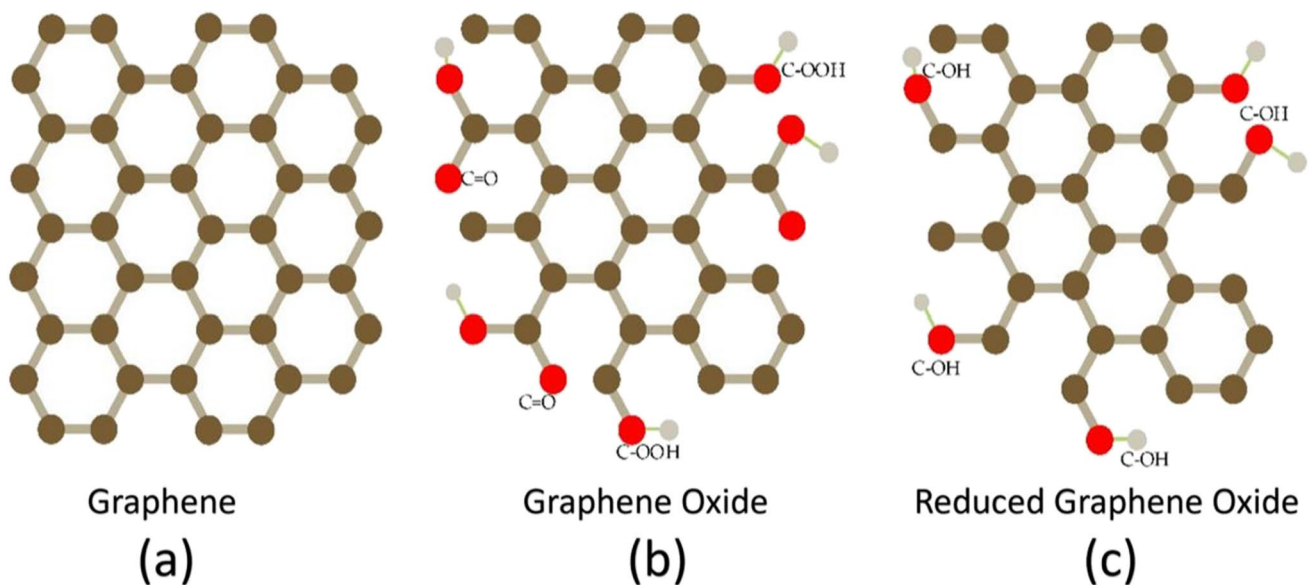


**Fig. 1** 2-Dimensional (a) graphene, (b) graphene oxide, (c) reduced graphene oxide

**Table 1** Different properties of rGO

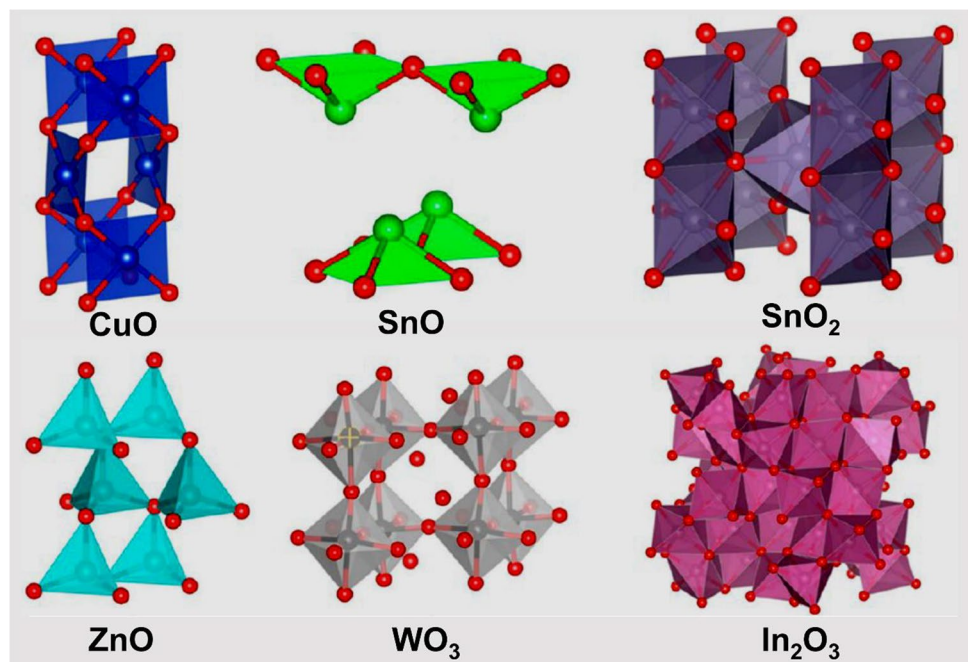
SI no	Properties		Ref
1	Mobility of charge carrier	250 000 cm <sup>2</sup> V <sup>-1</sup> s <sup>-1</sup>	[8]
2	Thermal conductivity	5000 Wm <sup>-1</sup> K <sup>-1</sup>	[9]
3	Electrical conductivity	6000 S cm <sup>-1</sup>	[10]
4	Specific surface area	2630 m <sup>2</sup> g <sup>-1</sup>	[11]

which exhibits higher electric conductivity compared to silver. The different properties of the rGO are listed in the Table 1.

MOs are a broad and attractive range of compounds with properties extending from metals to semiconductors and insulators, where metal oxide semiconductor (MOS) material with a narrow bandgap shows an adaptable range of properties, and it has been excellently used in the production of magnetic storage devices, gas-sensing, emission emitters, field-heterogeneous catalysis, lithium-ion electrode materials, photovoltaic devices, and optical and electrical devices [12]. MOS materials have been known for decades for their good electrical conductivities. Thus, the conductivity of semiconducting materials varies with the gas composition present around them. Yamazoe proved that sensor performance is significantly enhanced with reduction in crystallite size [13]. The enhanced sensing response with the reduction in size of MOs are attributed to the activation of more number of charge carriers from their trapped states to the conduction band upon the exposure to the target gases [14]. The controlled synthesis of MO nanoparticles is essential for different applications, due to the comparatively high

variation of their electrical resistance to adsorbent material, MO nanohybrid materials have been explored extensively as gas sensors [15]. Nanostructures of MO, such as Co<sub>3</sub>O<sub>4</sub>, Cu<sub>2</sub>O, Fe<sub>2</sub>O<sub>3</sub>, In<sub>2</sub>O<sub>3</sub>, TiO<sub>2</sub>, SnO<sub>2</sub>, WO<sub>3</sub>, and ZnO (see Fig. 2), have been widely used for sensing applications, due to their excellent chemical stability, mechanical flexibility, and large specific surface area [16]. The metal oxide nanoparticles have been chosen to study gas-sensing applications because of the following reasons: eco friendly MOs are used because of biosafe, biodegradable, and also biocompatible materials [17]. MO nanoparticles can be chosen by their structural properties with large surface to volume ratio and exhibits high mechanical strength, thermal stability, chemical stability, ambient insensibility, piezoelectric, and pyroelectric properties [18, 19]. The physical properties of MO nanoparticles exhibit an acute dependence on size. These properties are having special importance because these are related to the industrial use of oxides such as spintronics, sensors, catalysts, and absorbents. A bunch of novel applications within these fields are surely on the size dependence of the optical, charge transport, and surface or chemical properties of oxide nanomaterials. Size effects in oxides have frequently two interrelated faces: (a) structural or electronic quantum size and (b) size defect or non-stoichiometry effects.

MO nanoparticles have been intensively employed in diverse applications in the field of chemical and gas sensors, as CuO is attributed to a monoclinic crystal structure where each atoms are bounded to the four oxygen atoms in a rectangular parallelogram, in which Cu<sub>2</sub>O has received less attention towards gas-sensing applications than CuO. SnO and SnO<sub>2</sub> are attributed to many different structures in that

**Fig. 2** Crystal structures of metal oxides [20]

major structures are tetragonal and rutile which received much attention in the field of gas sensors. ZnO is attributed to hexagonal wurtzite structure for which Zn is bounded to the four O atoms which possess intrinsic defects like Zn interstitials and O vacancies, possessing distinct physico-chemical properties based on the rearrangement of positively and negatively charged on the surfaces; thus, these samples are employed in the field of gas sensor applications.  $\text{WO}_3$  has different crystal structures in that monoclinic structure and is most commonly explored for gas-sensing.  $\text{In}_2\text{O}_3$  is attributed to rhombohedral structure, which is highly conductive is commonly feasible to several applications. These MO particles have made into thick porous with a large surface area, and there are many drawbacks attributed in modifying the nanoparticles by its morphology, electrode design, dopants, and percentage dopants.

The pure MO nanoparticles have some disadvantages, while detecting some gases at low PPM and also, they are working at higher temperatures to overcome these problems the new materials are required to operate the gas sensors at room temperatures; thus, MO-doped with the different materials are used to overcome these problems. By increasing the sensitivity, favoring selective interactions with the target analyte increased selectivity and decreased response and recovery times, respectively; the proper doping process and material enhances sensor performance and lowers operating temperatures. Thus, to improvement sensing ability and synergetic enhancement of the two component systems, GO-MO-based nanocomposite materials have been proven from many literatures which can be used as gas-sensing materials due to its potential applications [21].

To improve the electrical and gas-sensing properties of the graphene, many MO ( $\text{ZnO}$ ,  $\text{WO}_3$ ,  $\text{SnO}_2$ ) nanoparticles are hybridized; however, gas sensors based on graphene-MO nanohybrids still have numerous drawbacks in terms of practical implementations such as the insufficient rate

of response, sensitivity, and extensive recovery time. Many recent efforts have been devoted to the controllable synthesis of 3D graphene-MO's architectures, owing to their large surface area and well-organized structure for enhanced gas adsorption/diffusion on sensing films, in order to achieve higher sensing performances of graphene-MO nanocomposites. Among all these, GO and MO nanoparticles have its own position among all the versatile materials, due to their diverse properties, functionalities, and many applications in different fields like catalysis, sensors, optoelectronic materials, and environmental remediation [22].

There are different techniques to functionalize rGO for various applications, by treating it to chemical or by combining it with other MO materials to form novel compounds as shown in Fig. 3. Thus, by modifying rGO, one can enhance the properties which are suitable for commercial applications. Functionalization of GO is crucial for regulating the exfoliation behavior of GO and rGO as well as revealing the key to a numerous application, including the improvement of conductivity and sensing abilities. MOs and rGO nanohybrid composites are extremely fascinating because of their additional synergistic characteristics that are desirable and efficient, in addition to the individual characteristics of the rGO and MO nanoparticles. One of the primary advantages of the composite gas sensors is that rGO possesses nearly metallic conductivity with the possibility of intrinsic detection of various gases. With the combination of MOs in rGO system due to the large specific surface area of graphene may have synergistic benefits for better gas response at room temperature, particularly in terms of selectivity and sensitivity. Graphene-based gas sensors have been investigated by many researchers that have been modified with a variety of metal oxides to create metal oxide-graphene nanohybrid sensors. However, the research has concentrated on graphene-based sensors in conjunction with MOs such as

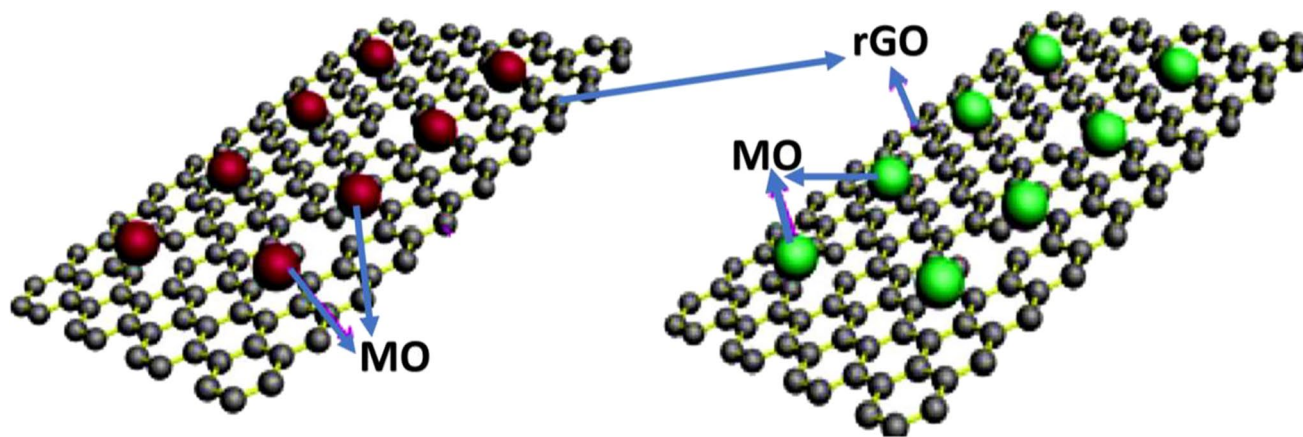


**Fig. 3** structural illustrations of reduced graphene oxide-metal oxide composites



$\text{WO}_3$ ,  $\text{Cu}_2\text{O}$ ,  $\text{Co}_3\text{O}_4$ ,  $\text{In}_2\text{O}_3$ , and  $\text{NiO}$  have also been explored to some extent. Many researchers have been working in this area, though an in-depth study about the effect of the compositions of rGO on the electrical and desired sensing properties of the composites is still deficient, but this field is still less explored.

## 2 Electrical properties of rGO-MO nanocomposites

MO materials are having wide band gap which is gaining a lot of attention for a variety of electrical and optoelectronic applications. The material having large band gap has several advantages, including high-power operation, withstand high temperature, greater breakdown voltages, decreased noise production, and the capacity to tolerate huge electric fields. Electron transport mechanism in MOS materials can be studied for both high and low electric fields. The majority of MOS materials exhibit electrical conductivity values that are similar to their thermal conductivity values. Typically, the ability of charge carriers and number of charge carriers of MOS were determined by the electrical conductivity characteristics, as increase in the temperature the movement of the charges becomes easier for the semiconductor materials to conduct charges. This is unique from metals, whereas the increase in temperature causes conductivity to decrease as a result of greater charge carrier scattering.

The conductivity of a semiconductor materials suddenly increases at a certain temperature because they undergo a semiconductor-to-metal transition; typically, this is caused by overlapping electron orbitals that form vacant d or f electron energy bands. The electronic behavior of a material becomes dominated by mechanisms at nanoscale, in which that are not factors when dealing with conventional semiconducting materials synthesized on the micron scale. In all semiconducting materials at the micron scale, one can see the existence of space charge layer, because of the size of the space charge layer in comparison with the bulk, and this is not a dominating mechanism with these larger grained materials. The materials are synthesized at the nanoscale, the fact that grain boundaries comprise to a large percentage of the materials which begins to control it electrical properties.

The MO nanoparticles decorated with graphene oxide have a low dielectric loss and high permittivity; the interfacial polarization between the MO nanoparticles and graphene layers has been improved. As a result, MO-decorated graphene plays a significant role in altering the characteristics of the graphene–MO nanocomposites [23]. Iskandar et al. have improved electrical conductivity of

rGO by microwave-assisted reduction method under nitrogen atmosphere [24].

The narrow band gap is found in rGO-MO composites, which is attributed to a stronger coupling between rGO sheets and MO nanoparticles, due to the smaller size and better distribution of MO on the graphene sheets [23]. Kuntal et al. have studied conductivity mechanism in rGO-ZnO nanocomposites at room temperature. The electrical conductivities of rGO-ZnO nanocomposites were found to decrease with the increase in the content of zinc oxide. Ahmed et al. have shown that  $\text{SnO}_2$ -rGO nanocomposites have enhanced AC conductivity, relatively low loss, and high dielectric constant in comparison to tin oxide ( $\text{SnO}_2$ ) [15]. Both types of the electrical conductivity, AC and DC; dielectric; optoelectronic; and thermal properties of  $\text{SnO}_2$ -rGO nanocomposites samples are significantly affected and can be controlled by the amount of the additive [25]. Darwish et al. studied about the influence of rGO on electrical and dielectric properties of  $\text{Co}_3\text{O}_4$ /rGO nanocomposites and found that gradual decrease in activation energy with increasing rGO content in MO [26]. The recent literatures reveals that rGO-MOs are the better materials having good class of electrical properties and electron transport phenomena.

## 3 Gas-sensing properties of rGO-MO nanocomposites

For the first time in 1953, Bardeen et al. discovered that gas adsorption on the surface of semiconductor material produces change in the conductivity [27]. Various metal oxide semiconductors (MOS), such as  $\text{PdO}$ ,  $\text{SnO}_2$ ,  $\text{Ni}_2\text{O}_3$ ,  $\text{ZnO}$ , are commonly used gas-sensing materials [28–33]. There are some disadvantages like poor selectivity, low sensitivity, and high working temperature are still great challenges associated with these MO sensors; to overcome these shortcomings and to enhance sensing characteristics, the alteration of MO by other elements, this has attracted considerable interest to prepare a new material [34].

The gas-sensing mechanism of rGO-MO nanocomposite is governed by many factors such as porosity of the sensing material, specific surface area, and formations of heterojunctions. MOS-based sensors work on the principle of the change in resistance owing to the reaction among gas molecules and the sensitive surface, which occurred on the surface of the sample with the method of adsorption and desorption. The oxygen molecules are adsorbed on the surface of the sample that are transformed to single/double ionized species by separating the electrons from the conduction band of the composite materials (see Fig. 4).

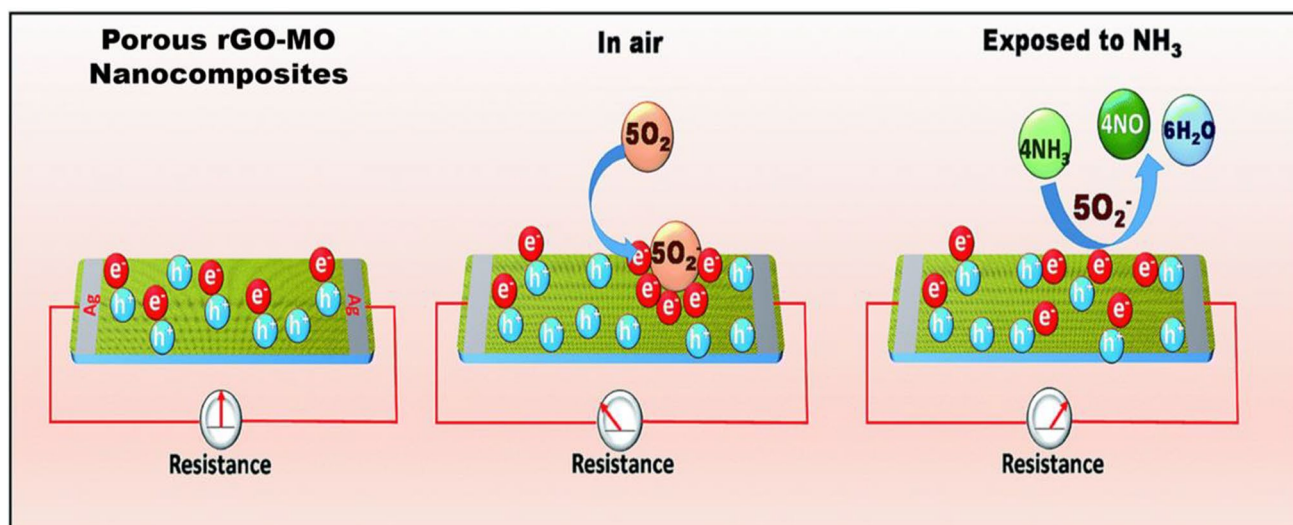


**Fig. 4** Schematic representation of the gas-sensing mechanism of the rGO-MO nanocomposite towards  $\text{NH}_3$  at room temperature [35]

Due to the transfer of electrons from the surface of composites to oxygen, the adsorbate oxygen generates a space charge layer, which results in the material's initial high resistance, this process is completely temperature-dependent (temperatures below  $100\text{ }^\circ\text{C}$  or at room temperature). A single molecular oxygen absorbs only one electron and forms a molecular ionic oxygen species ( $\text{O}_2^-$ ); but above  $100\text{ }^\circ\text{C}$ , it is capable of absorbing two electrons to form atomic oxygen species ( $\text{O}^-$  and  $\text{O}^{2-}$ ) [35]. The possible room temperature ammonia gas-sensing mechanism of rGO-MO composites is as follows:

For the room temperature, gas-sensing can make use of graphene, because of its extremely high carrier mobility. Nevertheless, the gas sensors based on pure graphene or rGO endure with some disadvantages, like such as long response time, low sensitivity, and recovery times, which are limited for some applications [21]. The development of gas sensors based on rGO-MO nanocomposites has received significant attention, due to the low sensitivity obtained by using MO nanoparticle gas sensor. In fact, some conventional MOs have been successfully used for enhancing the sensing properties of rGO-based gas sensors such as  $\text{SnO}_2$ ,  $\text{ZnO}$ ,  $\text{MoS}_2$ , and  $\text{WO}_3$  [36, 37].

NiO-sensing materials are the best candidate for practical application in selective detecting of benzaldehyde and that was observed by Yang et al., in terms of ion-adsorbed oxygen theory on the surface of the NiO material [38]. Naveen et al. studied for 10 vol% acetone and ethanol vapors in the presence of air at temperature range between  $373\text{--}573\text{ K}$  for the zinc oxide ( $\text{ZnO}$ ) samples. Among all the samples, fuel-to-oxidizer molar ratio of 1.7 has shown highest sensitivity to 10 vol% acetone and ethanol vapors in air at  $573\text{ K}$  [39, 40]. Gonzalez

et al. reported that the  $\text{In}_2\text{O}_3$ -based gas sensor shows high response at  $130\text{ }^\circ\text{C}$  for the  $\text{NO}_2$  gas, and the sensor response is less at  $240\text{ }^\circ\text{C}$  [42]. Titanium dioxide ( $\text{TiO}_2$ ) nanoparticles are used for the gas-sensing properties, many are working on this with different volume of analytes and for different temperatures, but the recovery time taken is very high even at higher temperatures [43–46]. Kida et al. investigated tungsten trioxide particles and studied  $\text{NO}_2$  gas-sensing properties of the material operated at high temperature [47]. The copper oxide ( $\text{CuO}$ ) particles are also having high potential applications to detect  $\text{NO}_2$  gas at higher operating temperature and shows good sensing properties was investigated by Li et al. [48]. Rajeeva et al. investigated the ethanol gas-sensing properties of  $\text{SnO}_2$ -thick films assembled by nanocrystals, which affected by the crystallite size, porosity of the sample, as the crystallite size increases the gas response decreases with decrease in porosity of the sample. At 2.5 volume % of ethanol, the sensing performance of sensor is 95% sensitivity influencing the activity of surface reaction [49]. Platinum-doped tin oxide enhances the gas sensors performance towards lower detection of CO. The gas-sensing performance can be tuned by varying the thickness of the film [51]. Trinchi et al. investigated the binary MO thin films using  $\text{CeO}_2\text{-TiO}_2$  for the different concentrations of oxygen gas; the samples shows good sensing performances below  $470\text{ }^\circ\text{C}$  [52].

Sharma et al. have studied the gas-sensing properties of GO and rGO samples using I–V characteristics, the results of the research suggests that both GO and rGO have the potential applications to be better gas-sensing material, with the surface of rGO is being more sensitive and corrugated than the surface of GO [73]. The GO-based gas sensors had

**Table 2** Gas-sensing properties of MOs, rGO, and rGO-MOs

SI no	Materials	Gas	Sensitivity/ response%	PPM/vol %	Response time	Recovery time	Temp	Ref
1	NiO	Benzaldehyde	46	10 PPM	37 (s)	38 (s)	300 °C	[38]
2	ZnO	Acetone	99.6%	10 vol%			300 °C	[39]
3	ZnO	Ethanol	99.4%	10 vol%			300 °C	[40]
4	Mg-In <sub>2</sub> O <sub>4</sub>	Oxygen		50PPB				[41]
5	In <sub>2</sub> O <sub>4</sub>	NO <sub>2</sub>	58	1000PPB			130 °C	[42]
6	Nb-TiO <sub>2</sub>	CO		1000PPM			650 °C	[43]
7	TiO <sub>2</sub>	Methanol			≈ 5 (s)		450 °C	[44]
8	TiO <sub>2</sub>	Acetone	140	50 PPM			RT	[45]
9	TiO <sub>2</sub>	Ethanol		100PPM			500 °C	[46]
10	WO <sub>3</sub>	NO <sub>2</sub>	90%	1000PPB	240 (s)	660 (s)	200 °C	[47]
11	CuO	NO <sub>2</sub>	2.2%	50PPM			200 °C	[48]
12	SnO <sub>2</sub>	Ethanol	95%	2.5 vol%			250 °C	[49]
13	SnO <sub>2</sub>	Ethanol	1000				450 °C	[50]
14	Pt-SnO <sub>2</sub>	CO	8	1 PPM			350 °C	[51]
15	CeO <sub>2</sub> -TiO <sub>2</sub>	O <sub>2</sub>	33%	10,000PPM	40–60 (s)	80 (s)	420 °C	[52]
16	GO	NO <sub>2</sub>	17%	5 PPM	900 (s)	1800 (s)	RT	[53]
17	Multi-layered graphene	Ammonia	55%	4000PPM			RT	[54]
18	Single-layered graphene	NO <sub>2</sub>	12%	1PPM			RT	[55]
19	Reduced GO	NO <sub>2</sub>	~ 12%	2PPM			RT	[56]
20	rGO	NH <sub>3</sub>	10.7	200PPM			RT	[57]
21	rGO	NO <sub>2</sub>	22%	50 PPM				[58]
22	rGO-TiO <sub>2</sub>	Ammonia	5%	30PPM			RT	[59]
23	rGO-SnO <sub>2</sub>	SO <sub>2</sub>	22%	500 PPM			60 °C	[60]
24	Graphene-WO <sub>3</sub>	NO <sub>2</sub>	133%	5 PPM	25 (s)	200 (s)	250 °C	[61]
25	GO-WO <sub>3</sub>	Alcohol	40.9%	2000 PPM			317 °C	[62]
26	rGO-WO <sub>3</sub>	NH <sub>3</sub>	11	100PPM			300 °C	[63]
27	rGO-ZnFe <sub>2</sub> O <sub>4</sub>	Acetone	8.18	10PPM			200 °C	[64]
28	rGO-Co <sub>3</sub> O <sub>4</sub>	NO <sub>2</sub>		60 PPM			RT	[65]
29	rGO-Co <sub>3</sub> O <sub>4</sub>	Ethanol	20%	10 PPM			200 °C	[66]
30	rGO-ZnO	NO <sub>2</sub>	680%	5 PPM			250 °C	[67]
		CH <sub>4</sub>	40%	500PPM				
		H <sub>2</sub>	30%	500PPM				
31	rGO-ZnO	NO <sub>2</sub>	25.6%	5 PPM	165 (s)	499 (s)	RT	[37]
32	rGO-ZnO	Methane	12.1	1000 PPM	~ 200 (s)		190 °C	[34]
33	rGO-NiO	NO <sub>2</sub>	~ 690%	15PPM			200 °C	[68]
34	rGO-Cu <sub>2</sub> O	NO <sub>2</sub>	67.8	2 PPM			RT	[69]
35	rGO-SnO <sub>2</sub>	Humidity	97 RH		102 (s)		RT	[70]
36	rGO-SnO <sub>2</sub>	NO <sub>2</sub>	4.63%	5 PPM	177 (s)	510 (s)	RT	[71]
37	Pd-SnO <sub>2</sub> -rGO	NH <sub>3</sub>	7.6%	5PPM	420 (s)	3000 (s)	RT	[72]

a high response and reversible properties for NO<sub>2</sub> gas, but the rGO and graphene-based gas sensors demonstrated lower responses and irreversible sensing operations; thus, it can be happened by the hydroxyl groups present in graphene and rGO [53]. It is believed that rGO materials would help in the development of cost-effective, large-area, flexible, and highly sensitive gas sensors which can be operated at room temperature [54, 56, 57]. Flexible graphene sensors provide

unrestricted size and design of sensor applications such as wearable nose-sensors and smart windows [55].

The results reported by Li et al. reveals the enhanced sensitivity to the different concentrations of ammonia from 5 to 50 PPM at room temperature [59]. Tyagi et al. synthesized MWCNT-SnO<sub>2</sub> and rGO-SnO<sub>2</sub> nanocomposite gas sensors by chemical method, for the pure SnO<sub>2</sub>-based sensor the sensing response of 1.2 is

obtained at 220 °C towards 500 PPM SO<sub>2</sub> gas, where rGO-SnO<sub>2</sub> sensor shows enhanced sensing response of ~ 22 at 60 °C and the MWCNT-SnO<sub>2</sub> sensor shown the sensing response of ~ 5 at a 60 °C for SO<sub>2</sub> gas at same concentrations [60].

Srivastava et al. was observed a highest sensing response for NO<sub>2</sub> gas at 250 °C temperature for graphene-WO<sub>3</sub> composites; the maximum value of sensor response was 133 for the nanocomposite of 0.5 wt% graphene doped to tungsten oxide (WO<sub>3</sub>) nanoparticles [61]. GO-WO<sub>3</sub> nanoparticle-based gas sensors are used in the alcohol detection but their operating temperature is high [62]. The rGO-WO<sub>3</sub> nanocomposite-based gas sensor is used to detect extremely hazardous NH<sub>3</sub> gas at low concentrations ranging from 20 to 500 PPM, and the highest response of 11 was recorded to 100 PPM of NH<sub>3</sub> gas. The developed gas sensors based on rGO-WO<sub>3</sub> nanocomposites offer substantial applications towards the environmental pollution monitoring systems [63]. The rGO was incorporated into the ZnFe<sub>2</sub>O<sub>4</sub> nanoparticles, enhanced the performance of acetone sensing at low concentrations, and the ZnFe<sub>2</sub>O<sub>4</sub>-rGO composite gas sensor containing 0.5 wt% rGO showed good sensitivity for 0.8–100 PPM acetone at 200 °C. The response of the 0.5 wt% ZnFe<sub>2</sub>O<sub>4</sub>-rGO sensor to 0.8 PPM acetone was 1.50, and for 10 PPM acetone was 8.18, which is higher than the pure ZnFe<sub>2</sub>O<sub>4</sub> sensor [64].

The Co<sub>3</sub>O<sub>4</sub>-rGO composite-based gas sensors had a considerably greater response to NO<sub>2</sub> at room temperature, compared to pure rGO sensors. However, as the concentration of rGO increases from 5 to 30 wt%, the reaction exhibited a declining trend, due to the considerable strong adsorption of NO<sub>2</sub> at the defective sites of rGO, the sensor response to NO<sub>2</sub> was not entirely recoverable during the measurement time. In contrast to the rGO-based gas sensors showed a quick response and complete recovery to methanol vapors; thus, it has been exclusively proposed to the interaction of methanol with the sp<sup>2</sup> bonding of carbon. Similarly, the response of cobalt oxide (Co<sub>3</sub>O<sub>4</sub>) intercalated rGO was significantly enhanced the response/recovery time of within 1–2 min for the methanol vapor [65]. Tian et al. also investigated gas-sensing performances of the rGO-Co<sub>3</sub>O<sub>4</sub> composites to several VOCs, showed long-term stability, excellent circularity, and high response is recorded for 10 PPM of ethanol vapors at 200 °C, and the sample with 15 wt% of rGO exhibited the best sensitivity [66]. Galstyan et al. have been demonstrated that the rGO/ZnO composites exhibit 40–50% better response to NO<sub>2</sub> and H<sub>2</sub> compared to pure ZnO sensors [67].

We believe that rGO-MO hybrid nanocomposites can be effectively used in many types of gas-sensing applications due to its simple processing and superior performance [68]. Deng et al. prepared the rGO-Cu<sub>2</sub>O meso-crystals of high specific surface area, and the samples show higher

sensitivity toward NO<sub>2</sub> at room temperature than that of individual ones [69]. Zhang et al. reported the humidity-sensing abilities of the SnO<sub>2</sub>/rGO nanohybrid sensor that were studied by exposing it into a wide range of humidity (11–97%) at room temperature; these sensors were having ultra-high sensitivity and a rapid response or recovery time when compared with traditional humidity sensors [70].

Latif et al. have discussed about the advantages of graphene hybrid materials for gas-sensing applications, and many more researchers have studied the rGO-MOS composite materials as chemiresistive gas sensors [67, 74, 75]. However, these gas sensors still suffer from several shortcomings, such as high-operating temperature, long response and recovery times, low sensitivity, and selectivity. It is evident from the earlier reports (Table 2) that MO's hybridize with rGO can be used as chemiresistive gas sensors. The rGO-MO nanocomposites are the better alternatives for the nanomaterial-based gas sensors due to many promising and unique properties.

## 4 Conclusion

This article summarizes the properties of rGO-MO nanocomposites, which are used to detect various gases from lower PPM to higher PPM levels. Hybrid materials have high sensitivity and more suitable for room temperature operation than individual components. MOs are conducting/semiconducting materials with narrow bandgaps, those can exhibit a wide range of properties, and rGOs are more significant than similar carbon derivatives because of their unique and distinctive characteristics. The electrical properties of rGO-MO nanocomposites have been improved with the variation in concentrations of the MOs in rGO at room temperature. The rGO-MO composites are good sensing materials due to their higher surface to volume ratio; therefore, one can expect increased sensitivity towards hazardous gases. The rGO-MO composites show enhanced selectivity, sensitivity, and stability at room temperature, thereby avoids the power consumption for the operation of sensors. One could fabricate portable sensor devices from rGO-MO composites, which are compatible to sense various gases with strong mechanical excellence.

**Author contribution** Kirannakumar H. V, Thejas R, Naveen C S and Mowffaq Oreijah work on literature survey; M. Ijaz Khan and Kirannakumar H. V. computed the results; Prasanna G. D and Kamel Guedri write the final manuscript; M. Ijaz Khan, Kamel Guedri, Omar T Bafakeeh, and Mohammed Jameel work on the figure illustration and address the referee's comments. Sathish Reddy and M. Ijaz Khan review the final version.



**Funding** The authors would like to thank the Deanship of Scientific Research at Umm Al-Qura University for supporting this work by Grant Code: 22UQU4340474DSR04. The authors extend their appreciation to the deanship of scientific research at King Khalid University for funding this work through large group project under grant number (RGP. 2/83/43).

**Data availability** All the data are available in the research work.

## Declarations

**Competing interests** The authors declare no competing interests.

## References

- Paul DR, Robeson LM (2008) Polymer nanotechnology: nanocomposites. *Polymer* 49:3187–3204. <https://doi.org/10.1016/j.polymer.2008.04.017>
- Ealia SAM, Saravanakumar MP (2017) A review on the classification, characterisation, synthesis of nanoparticles and their application. *IOP Conf Ser Mater Sci Eng* 263:032019. <https://doi.org/10.1088/1757-899X/263/3/032019>
- Jeevanandam J, Barhoum A, Chan YS, Dufresne A, Danquah MK (2018) Review on nanoparticles and nanostructured materials: history, sources, toxicity and regulations. *Beilstein J Nanotechnol* 9:1050–1074. <https://doi.org/10.3762/bjnano.9.98>
- Saifuddin N, Raziah AZ, Junizah AR (2012) Carbon nanotubes: a review on structure and their interaction with proteins. *J Chem* 2013:e676815. <https://doi.org/10.1155/2013/676815>
- MM Azim, U Mohsin, 2019 Chapter 7 - Graphene oxide/transition metal oxide as a promising nanomaterial for hydrogen storage, in: M. Jawaid, A. Ahmad, D. Lokhat (Eds.), *Graphene-Based Nanotechnologies Energy Environ. Appl.*, Elsevier, 121–144. <https://doi.org/10.1016/B978-0-12-815811-1.00007-7>.
- Wu J, Pisula W, Müllen K (2007) Graphenes as potential material for electronics. *Chem Rev* 107:718–747. <https://doi.org/10.1021/cr068010r>
- AK Geim, K.S. Novoselov, 2009 The rise of graphene, *Nanosci. Technol. Collect. Rev. Nat. J.* 11–19. [https://doi.org/10.1142/9789814287005\\_0002](https://doi.org/10.1142/9789814287005_0002).
- Orlita M, Faugeras C, Plochocka P, Neugebauer P, Martinez G, Maude DK, Barra AL, Sprinkle M, Berger C, De Heer WA, Potemski M (2008) Approaching the dirac point in high-mobility multilayer epitaxial graphene. *Phys Rev Lett* 101:1–4. <https://doi.org/10.1103/PhysRevLett.101.267601>
- Balandin AA, Ghosh S, Bao W, Calizo I, Teweldebrhan D, Miao F, Lau CN (2008) Superior thermal conductivity of single-layer graphene. *Nano Lett* 8:902–907. <https://doi.org/10.1021/nl0731872>
- Du X, Skachko I, Barker A, Andrei EY (2008) Approaching ballistic transport in suspended graphene. *Nat Nanotechnol* 3:491–495. <https://doi.org/10.1038/nnano.2008.199>
- Zhu Y, Murali S, Cai W, Li X, Suk JW, Potts JR, Ruoff RS (2010) Graphene and graphene oxide: synthesis, properties, and applications. *Adv Mater* 22:3906–3924. <https://doi.org/10.1002/adma.201001068>
- Reddy S, Kumara Swamy BE, Jayadevappa H (2012) CuO nanoparticle sensor for the electrochemical determination of dopamine. *Electrochimica Acta.* 61:78–86. <https://doi.org/10.1016/j.electacta.2011.11.091>
- Yamazoe N (1991) New approaches for improving semiconductor gas sensors. *Sens Actuators B Chem* 5:7–19. [https://doi.org/10.1016/0925-4005\(91\)80213-4](https://doi.org/10.1016/0925-4005(91)80213-4)
- S. Khaldi, Z. Dibi, 2017 Neural network modeling of smart nano-structure sensor for electronic nose application, in: 2017 6th Int. Conf. Syst. Control ICSC, pp. 607–610. <https://doi.org/10.1109/ICoSC.2017.7958690>
- Prinz GA (1998) Magnetoelectronics. *Science* 282:1660–1663. <https://doi.org/10.1126/science.282.5394.1660>
- Sun D, Luo Y, Debliqy M, Zhang C (2018) Graphene-enhanced metal oxide gas sensors at room temperature: a review. *Beilstein J Nanotechnol* 9:2832–2844. <https://doi.org/10.3762/bjnano.9.264>
- Story T, Gałazka RR, Frankel RB, Wolff PA (1986) Carrier-concentration induced ferromagnetism in PbSnMnTe. *Phys Rev Lett* 56:777–779. <https://doi.org/10.1103/PhysRevLett.56.777>
- DJ Heinzen, RH Wynar, PD Kheruntsyan, PD Drummond, T Dietl, H Ohno, F Matsukura, J Cibert, D Ferrand, 1995 Zener model description of ferromagnetism in zinc-blende magnetic semiconductors Downloaded from. *Chem Phys Lett* 269; 2657
- Zener C (1951) Interaction between the d shells in the transition metals. *Phys Rev* 81:440–444. <https://doi.org/10.1103/PhysRev.81.440>
- Yoon Y, Truong PL, Lee D, Ko SH (2022) Metal-oxide nanomaterials synthesis and applications in flexible and wearable sensors. *ACS Nanosci Au* 2:64–92. <https://doi.org/10.1021/acsnanosci.1c00029>
- Tian W, Liu X, Yu W (2018) Research progress of gas sensor based on graphene and its derivatives: a review. *Appl Sci* 8:1118. <https://doi.org/10.3390/app8071118>
- J.K. Furdyna, Diluted magnetic semiconductors, 29 (2012). <https://doi.org/10.1063/1.341700>.
- Ahmed A, Siddique MN, Ali T, Tripathi P (2018) Influence of reduced graphene oxide on structural, optical, thermal and dielectric properties of SnO<sub>2</sub> nanoparticles. *Adv Powder Technol* 29:3415–3426. <https://doi.org/10.1016/j.apt.2018.09.026>
- Iskandar F, Hikmah U, Stavila E, Aimon AH (2017) Microwave-assisted reduction method under nitrogen atmosphere for synthesis and electrical conductivity improvement of reduced graphene oxide (rGO). *RSC Adv* 7:52391–52397. <https://doi.org/10.1039/C7RA10013B>
- Aydın C (2019) Synthesis of SnO<sub>2</sub>:rGO nanocomposites by the microwave-assisted hydrothermal method and change of the morphology, structural, optical and electrical properties. *J Alloys Compd* 771:964–972. <https://doi.org/10.1016/j.jallcom.2018.08.298>
- Darwish AG, Ghoneim AM, Hassaan MY, Shehata OS, Turkey GM (2019) Impact of RGO on electrical and dielectric properties of Co<sub>3</sub>O<sub>4</sub>/RGO nanocomposite. *Mater Res Express* 6:105039. <https://doi.org/10.1088/2053-1591/ab3999>
- Brattain WH, Bardeen J (1953) Surface properties of germanium. *Bell Syst Tech J* 32:1–41. <https://doi.org/10.1002/j.1538-7305.1953.tb01420.x>
- Jiménez-Cadena G, Riu J, Rius FX (2007) Gas sensors based on nanostructured materials. *Analyst* 132:1083–1099. <https://doi.org/10.1039/B704562J>
- Nazemi H, Joseph A, Park J, Emadi A (2019) Advanced micro- and nano-gas sensor technology: a review. *Sensors* 19:1285. <https://doi.org/10.3390/s19061285>
- Patil SL, Chougule MA, Pawar SG, Sen S, Moholkar AV, Kim JH, Patil VB (2011) Fabrication of polyaniline-ZnO nanocomposite gas sensor. *Sens Transducers* 134:120–131
- Prajesh R, Jain N, Agarwal A (2016) Low power highly sensitive platform for gas sensing application. *Microsyst Technol* 22:2185–2192. <https://doi.org/10.1007/s00542-015-2609-1>
- Pramod NG, Pandey SN, Sahay PP (2012) Structural, optical and methanol sensing properties of sprayed In<sub>2</sub>O<sub>3</sub> nanoparticle thin

- films. *Ceram Int* 38:4151–4158. <https://doi.org/10.1016/j.ceramint.2012.01.075>
33. Wang L, Kalyanasundaram K, Stanacevic M, Gouma P (2010) Nanosensor device for breath acetone detection. *Sens Lett* 8:709–712. <https://doi.org/10.1166/sl.2010.1334>
  34. Zhang D, Yin N, Xia B (2015) Facile fabrication of ZnO nanocrystalline-modified graphene hybrid nanocomposite toward methane gas sensing application. *J Mater Sci Mater Electron* 26:5937–5945. <https://doi.org/10.1007/s10854-015-3165-2>
  35. Jeevitha G, Abhinayaa R, Mangalaraj D, Ponpandian N, Meena P, Mounasamy V, Madanagurusamy S (2019) Porous reduced graphene oxide (rGO)/WO<sub>3</sub> nanocomposites for the enhanced detection of NH<sub>3</sub> at room temperature. *Nanoscale Adv* 1:1799–1811. <https://doi.org/10.1039/C9NA00048H>
  36. Donarelli M, Ottaviano L (2018) 2D materials for gas sensing applications: a review on graphene oxide, MoS<sub>2</sub>, WS<sub>2</sub> and phosphorene. *Sensors* 18:3638. <https://doi.org/10.3390/s18113638>
  37. Liu S, Yu B, Zhang H, Fei T, Zhang T (2014) Enhancing NO<sub>2</sub> gas sensing performances at room temperature based on reduced graphene oxide-ZnO nanoparticles hybrids. *Sens Actuators B Chem* 202:272–278. <https://doi.org/10.1016/j.snb.2014.05.086>
  38. Yang F, Guo Z (2016) Engineering NiO sensitive materials and its ultra-selective detection of benzaldehyde. *J Colloid Interface Sci* 467:192–202. <https://doi.org/10.1016/j.jcis.2016.01.033>
  39. Naveen CS, MP Rajeeva, AR Lamani, HS. Jayanna, 2014 Acetone sensing properties of ZnO nanomaterial, in: Proc. Natl. Conf. Recent Trends Physics Mathematics Eng. Mysore
  40. Naveen CS, Rajeeva MP, Ashok RL, Jayanna HS (2017) Influence of crystallite size on ethanol sensing properties of ZnO nanomaterials. *Mater Today Proc* 4:12032–12038. <https://doi.org/10.1016/j.matpr.2017.09.127>
  41. Rombach J, Bierwagen O, Papadogianni A, Mischo M, Cimalla V, Berthold T, Krischok S, Himmerlich M (2015) Electrical conductivity and gas-sensing properties of Mg-doped and undoped single-crystalline In<sub>2</sub>O<sub>3</sub> thin films: bulk vs. surface. *Procedia Eng.* 120:79–82. <https://doi.org/10.1016/j.proeng.2015.08.570>
  42. O Gonzalez, S Roso, R Calavia, X Vilanova, E Llobet, 2015 NO<sub>2</sub> sensing properties of thermally or UV activated In<sub>2</sub>O<sub>3</sub> nano-octahedra. <https://doi.org/10.1016/J.PROENG.2015.08.817>
  43. Anukunprasert T, Saiwan C, Traversa E (2005) The development of gas sensor for carbon monoxide monitoring using nanostructure of Nb–TiO<sub>2</sub>. *Sci Technol Adv Mater* 6:359–363. <https://doi.org/10.1016/j.stam.2005.02.020>
  44. Benkstein KD, Semancik S (2006) Mesoporous nanoparticle TiO<sub>2</sub> thin films for conductometric gas sensing on microhotplate platforms. *Sens Actuators B Chem* 113:445–453. <https://doi.org/10.1016/j.snb.2005.03.122>
  45. Avinash BS, Chaturmukha VS, Harish BM, Jayanna HS, Rajeeva MP, Naveen CS, Lamani AR (2018) Synthesis, Characterization and room temperature acetone sensing of TiO<sub>2</sub> nanotubes. *Sens Lett* 16:105–109. <https://doi.org/10.1166/sl.2018.3921>
  46. Garzella C, Comini E, Tempesti E, Frigeri C, Sberveglieri G (2000) TiO<sub>2</sub> thin films by a novel sol–gel processing for gas sensor applications. *Sens Actuators B Chem* 68:189–196. [https://doi.org/10.1016/S0925-4005\(00\)00428-7](https://doi.org/10.1016/S0925-4005(00)00428-7)
  47. Kida T, Nishiyama A, Yuasa M, Shimano K, Yamazoe N (2009) Highly sensitive NO<sub>2</sub> sensors using lamellar-structured WO<sub>3</sub> particles prepared by an acidification method. *Sens Actuators B Chem* 135:568–574. <https://doi.org/10.1016/j.snb.2008.09.056>
  48. Li Y, Liang J, Tao Z, Chen J (2008) CuO particles and plates: synthesis and gas-sensor application. *Mater Res Bull* 43:2380–2385. <https://doi.org/10.1016/j.materresbull.2007.07.045>
  49. Rajeeva MP, Naveen CS, Lamani AR, Jayanna HS (2017) Synthesis, characterization and electrical conductivity of high porous tin oxide nanocrystallites for ethanol sensing. *Mater Today Proc* 4:12094–12102. <https://doi.org/10.1016/j.matpr.2017.09.136>
  50. Llobet E, Ivanov P, Vilanova X, Brezmes J, Hubalek J, Malysz K, Gràcia I, Cané C, Correig X (2003) Screen-printed nanoparticle tin oxide films for high-yield sensor microsystems. *Sens Actuators B Chem* 96:94–104. [https://doi.org/10.1016/S0925-4005\(03\)00491-X](https://doi.org/10.1016/S0925-4005(03)00491-X)
  51. Mädler L, Roessler A, Pratsinis SE, Sahn T, Gurlo A, Barsan N, Weimar U (2006) Direct formation of highly porous gas-sensing films by in situ thermophoretic deposition of flame-made Pt/SnO<sub>2</sub> nanoparticles. *Sens Actuators B Chem* 114:283–295. <https://doi.org/10.1016/j.snb.2005.05.014>
  52. Trinchì A, Li YX, Wlodarski W, Kaciulis S, Pandolfi L, Viticoli S, Comini E, Sberveglieri G (2003) Investigation of sol–gel prepared CeO<sub>2</sub>–TiO<sub>2</sub> thin films for oxygen gas sensing. *Sens Actuators B Chem* 95:145–150. [https://doi.org/10.1016/S0925-4005\(03\)00424-6](https://doi.org/10.1016/S0925-4005(03)00424-6)
  53. Choi YR, Yoon Y-G, Choi KS, Kang JH, Shim Y-S, Kim YH, Chang HJ, Lee J-H, Park CR, Kim SY, Jang HW (2015) Role of oxygen functional groups in graphene oxide for reversible room-temperature NO<sub>2</sub> sensing. *Carbon* 91:178–187. <https://doi.org/10.1016/j.carbon.2015.04.082>
  54. Ghosh R, Singh A, Santra S, Ray SK, Chandra A, Guha PK (2014) Highly sensitive large-area multi-layered graphene-based flexible ammonia sensor. *Sens Actuators B Chem* 205:67–73. <https://doi.org/10.1016/j.snb.2014.08.044>
  55. Choi H, Choi JS, Kim J-S, Choe J-H, Chung KH, Shin J-W, Kim JT, Youn D-H, Kim K-C, Lee J-I, Choi S-Y, Kim P, Choi C-G, Yu Y-J (2014) Flexible and Transparent gas molecule sensor integrated with sensing and heating graphene layers. *Small* 10:3685–3691. <https://doi.org/10.1002/sml.201400434>
  56. Lu G, Ocola LE, Chen J (2009) Reduced graphene oxide for room-temperature gas sensors. *Nanotechnology* 20:445502. <https://doi.org/10.1088/0957-4484/20/44/445502>
  57. Su P-G, Shieh H-C (2014) Flexible NO<sub>2</sub> sensors fabricated by layer-by-layer covalent anchoring and in situ reduction of graphene oxide. *Sens Actuators B Chem* 190:865–872. <https://doi.org/10.1016/j.snb.2013.09.078>
  58. Yuan W, Liu A, Huang L, Li C, Shi G (2013) High-performance NO<sub>2</sub> sensors based on chemically modified graphene. *Adv Mater* 25:766–771. <https://doi.org/10.1002/adma.201203172>
  59. Li X, Zhao Y, Wang X, Wang J, Gaskov AM, Akbar SA (2016) Reduced graphene oxide (rGO) decorated TiO<sub>2</sub> microspheres for selective room-temperature gas sensors. *Sens Actuators B Chem* 230:330–336. <https://doi.org/10.1016/j.snb.2016.02.069>
  60. Tyagi P, Sharma A, Tomar M, Gupta V (2017) A comparative study of RGO-SnO<sub>2</sub> and MWCNT-SnO<sub>2</sub> nanocomposites based SO<sub>2</sub> gas sensors. *Sens Actuators B Chem* 248:980–986. <https://doi.org/10.1016/j.snb.2017.02.147>
  61. Srivastava S, Jain K, Singh VN, Singh S, Vijayan N, Dilawar N, Gupta G, Senguttuvan TD (2012) Faster response of NO<sub>2</sub> sensing in graphene–WO<sub>3</sub> nanocomposites. *Nanotechnology* 23:205501. <https://doi.org/10.1088/0957-4484/23/20/205501>
  62. Qin J, Cao M, Li N, Hu C (2011) Graphene-wrapped WO<sub>3</sub> nanoparticles with improved performances in electrical conductivity and gas sensing properties. *J Mater Chem* 21:17167–17174. <https://doi.org/10.1039/C1JM12692J>
  63. Hung CM, Dat DQ, Van Duy N, Van Quang V, Van Toan N, Van Hieu N, Hoa ND (2020) Facile synthesis of ultrafine rGO/WO<sub>3</sub> nanowire nanocomposites for highly sensitive toxic NH<sub>3</sub> gas sensors. *Mater Res Bull* 125:110810. <https://doi.org/10.1016/j.materresbull.2020.110810>
  64. Wu K, Luo Y, Li Y, Zhang C (2019) Synthesis and acetone sensing properties of ZnFe<sub>2</sub>O<sub>4</sub>/rGO gas sensors. *Beilstein J Nanotechnol* 10:2516–2526. <https://doi.org/10.3762/bjnano.10.242>

65. Chen N, Li X, Wang X, Yu J, Wang J, Tang Z, Akbar SA (2013) Enhanced room temperature sensing of Co<sub>3</sub>O<sub>4</sub>-intercalated reduced graphene oxide based gas sensors. *Sens Actuators B Chem* 188:902–908. <https://doi.org/10.1016/j.snb.2013.08.004>
66. Tian M, Miao J, Cheng P, Mu H, Tu J, Sun J (2019) Layer-by-layer nanocomposites consisting of Co<sub>3</sub>O<sub>4</sub> and reduced graphene (rGO) nanosheets for high selectivity ethanol gas sensors. *Appl Surf Sci* 479:601–607. <https://doi.org/10.1016/j.apsusc.2019.02.148>
67. Galstyan V, Comini E, Kholmanov I, Faglia G, Sberveglieri G (2016) Reduced graphene oxide/ZnO nanocomposite for application in chemical gas sensors. *RSC Adv* 6:34225–34232. <https://doi.org/10.1039/C6RA01913G>
68. Hoa LT, Tien HN, Luan VH, Chung JS, Hur SH (2013) Fabrication of a novel 2D-graphene/2D-NiO nanosheet-based hybrid nanostructure and its use in highly sensitive NO<sub>2</sub> sensors. *Sens Actuators B Chem* 185:701–705. <https://doi.org/10.1016/j.snb.2013.05.050>
69. Deng S, Tjoa V, Fan HM, Tan HR, Sayle DC, Olivo M, Mhaisalkar S, Wei J, Sow CH (2012) Reduced graphene oxide conjugated Cu<sub>2</sub>O nanowire mesocrystals for high-performance NO<sub>2</sub> gas sensor. *J Am Chem Soc* 134:4905–4917. <https://doi.org/10.1021/ja211683m>
70. Zhang D, Chang H, Li P, Liu R, Xue Q (2016) Fabrication and characterization of an ultrasensitive humidity sensor based on metal oxide/graphene hybrid nanocomposite. *Sens Actuators B Chem* 225:233–240. <https://doi.org/10.1016/j.snb.2015.11.024>
71. Zhang H, Feng J, Fei T, Liu S, Zhang T (2014) SnO<sub>2</sub> nanoparticles-reduced graphene oxide nanocomposites for NO<sub>2</sub> sensing at low operating temperature. *Sens Actuators B Chem* 190:472–478. <https://doi.org/10.1016/j.snb.2013.08.067>
72. Su P-G, Yang L-Y (2016) NH<sub>3</sub> gas sensor based on Pd/SnO<sub>2</sub>/RGO ternary composite operated at room-temperature. *Sens Actuators B Chem* 223:202–208. <https://doi.org/10.1016/j.snb.2015.09.091>
73. Sharma N, Sharma V, Jain Y, Kumari M, Gupta R, Sharma SK, Sachdev K (2017) Synthesis and characterization of graphene oxide (GO) and reduced graphene oxide (rGO) for gas sensing application. *Macromol Symp* 376:1700006. <https://doi.org/10.1002/masy.201700006>
74. Latif U, Dickert FL (2015) Graphene hybrid materials in gas sensing applications. *Sensors* 15:30504–30524. <https://doi.org/10.3390/s151229814>
75. Cao Y, Li Y, Jia D, Xie J (2014) Solid-state synthesis of SnO<sub>2</sub>-graphene nanocomposite for photocatalysis and formaldehyde gas sensing. *RSC Adv* 4:46179–46186. <https://doi.org/10.1039/C4RA06995A>

**Publisher's note** Springer Nature remains neutral with regard to jurisdictional claims in published maps and institutional affiliations.

Springer Nature or its licensor holds exclusive rights to this article under a publishing agreement with the author(s) or other rightsholder(s); author self-archiving of the accepted manuscript version of this article is solely governed by the terms of such publishing agreement and applicable law.